



Title	Atomic structures of Ag <sub>2</sub> Te studied by scanning tunneling microscopy
Author(s)	Ohto, M.; Tanaka, K.
Citation	Journal of Vacuum Science & Technology B: Microelectronics and Nanometer Structures, 14(6), 3452-3454 <a href="https://doi.org/10.1116/1.588778">https://doi.org/10.1116/1.588778</a>
Issue Date	1996-11
Doc URL	<a href="http://hdl.handle.net/2115/5828">http://hdl.handle.net/2115/5828</a>
Type	article
File Information	JVS&TB14-6.pdf



[Instructions for use](#)

# Atomic structures of Ag<sub>2</sub>Te studied by scanning tunneling microscopy

M. Ohto and K. Tanaka<sup>a)</sup>

*Department of Applied Physics, Faculty of Engineering, Hokkaido University, Sapporo 060, Japan*

(Received 23 February 1996; accepted 30 August 1996)

Atomic structures of Ag<sub>2</sub>Te in the low- and high-temperature phases have been studied using a scanning tunneling microscope in air and an x-ray diffraction system. In the low-temperature phase having a monoclinic lattice, (001) and (010) atomic images are obtained. In the superionic high-temperature phase, which is stable at temperatures above 145 °C, (100) surfaces of the Te cubic lattice are observed. In both phases, surface atomic reconstructions are not detected. © 1996 American Vacuum Society.

## I. INTRODUCTION

Ag-chalcogenide crystals have been the subject of detailed experimental and theoretical studies for a long time because of the superionic properties observed at relatively low temperatures.<sup>1,2</sup> For instance, Ag<sub>2</sub>Te exhibits a structural phase transition from a low- to a high-temperature phase at around 145 °C,<sup>3</sup> which accompanies a jumpwise increase in the Ag ionic conductivity from 10<sup>-3</sup> S/cm to a superionic level of 10<sup>0</sup> S/cm.<sup>2</sup> The crystalline structure is monoclinic in the low-temperature phase.<sup>4</sup> In the high-temperature phase, it is cubic, and Te anions form a face centered cubic (fcc) sublattice<sup>4</sup> through which Ag cations can move easily, thus giving rise to the superionic conductivity.<sup>2,5</sup> In contrast, the electronic conductivity remains mostly constant at a relatively high value, 10<sup>2</sup>–10<sup>3</sup> S/cm, which can be ascribed to a degenerate *n*-type conduction.<sup>6</sup> Accordingly, Ag<sub>2</sub>Te may also be regarded as a mixed ionic-electronic conductor for the whole temperature range.<sup>1,2</sup>

Despite the interesting ionic property, little is known about the atomic surface structure of Ag-chalcogenide materials. So far, surface structures and modifications of amorphous Ag–Ge–Se films have been studied using scanning tunneling microscopes (STMs),<sup>7,8</sup> where the studies deal with nanometer-size structures. Although atomic images of ionic crystals such as NaCl and AgBr have been obtained by atomic force microscopy (AFM),<sup>9,10</sup> further studies are interesting for ionic materials, specifically ion-conducting materials.

Therefore, we decided to investigate the atomic surface structure of Ag-chalcogenide crystals, particularly in the superionic phase. Because high electronic conductivity is favorable for STM observations, Ag<sub>2</sub>Te was felt to be an appropriate choice for this study. We will show the first atomic image of the mixed ionic-electronic conductor in the normal and the superionic phase.

## II. EXPERIMENT

Film and bulk forms of Ag<sub>2</sub>Te were investigated in the present study. Film samples were synthesized by annealing Te/Ag bilayer films. First, atomically flat Ag films with a

thickness of 1000–2000 Å were grown by evaporating Ag pellets onto mica substrates heated at ~200 °C, the conditions being previously reported.<sup>11</sup> The Ag films were confirmed to have (111) orientation by x-ray diffraction and STM observations. Te films were then deposited to a thickness of ~100 Å. By annealing this bilayer film in an Ar gas at 400 °C for 3 h, Ag and Te reacted and changed into Ag<sub>2</sub>Te. Polycrystalline Ag<sub>2</sub>Te was synthesized by melting a stoichiometric mixture of the elements with six-nine purity in an evacuated silica tube. The sample was held at 1000 °C for 11 h, and then slowly cooled to room temperature in a furnace.

Sample surfaces were inspected using a commercial STM equipment (Digital Instrument, Nanoscope III) slightly customized for use at variable temperatures. A resistive heater (5×5×1 mm size) was mounted on the base plate on which a sample was fixed. Mechanically sharpened PtIr wires were utilized as scanning tips. The sample and the tip were covered by silicone oil (Toshiba silicone 951A), which acts to suppress surface oxidation<sup>12</sup> and mechanical vibration as well. The sample temperature was monitored using a small thermocouple attached near the sample. In order to suppress thermal drift arising from heat conduction and air convection, the sample-tip assembly was covered with a small Cu shield case. The thermal drift of this system at 150 °C was estimated at ~2 Å/s by inspecting a surface of highly oriented pyrolytic graphite.

Subsidiary measurements were performed using an x-ray diffraction system. The system consisted of a rotating Cu anode operating at 50 kV and 250 mA (Rigaku RU-300), a variable-temperature sample cell which was attached to a diffractometer stage, a scintillation counter fitted with a graphite monochromator, and a computer.

## III. RESULTS AND DISCUSSION

Figure 1(a) shows a typical x-ray diffraction pattern of Ag<sub>2</sub>Te films at room temperature. In Fig. 1, the prominent peaks marked with cross and triangle symbols are due to the mica substrate and unreacted Ag metal. Also, a halo peak located around 2θ=25° is caused by a slide-glass plate which holds the sample. The Ag<sub>2</sub>Te film is estimated to be thin (~100 Å); it gives two small peaks which are indicated by arrows and indexed according to previous studies.<sup>4,13</sup>

<sup>a)</sup>Author to whom correspondence should be addressed; Electronic mail: keiji@hikari4.huap.hokudai.ac.jp

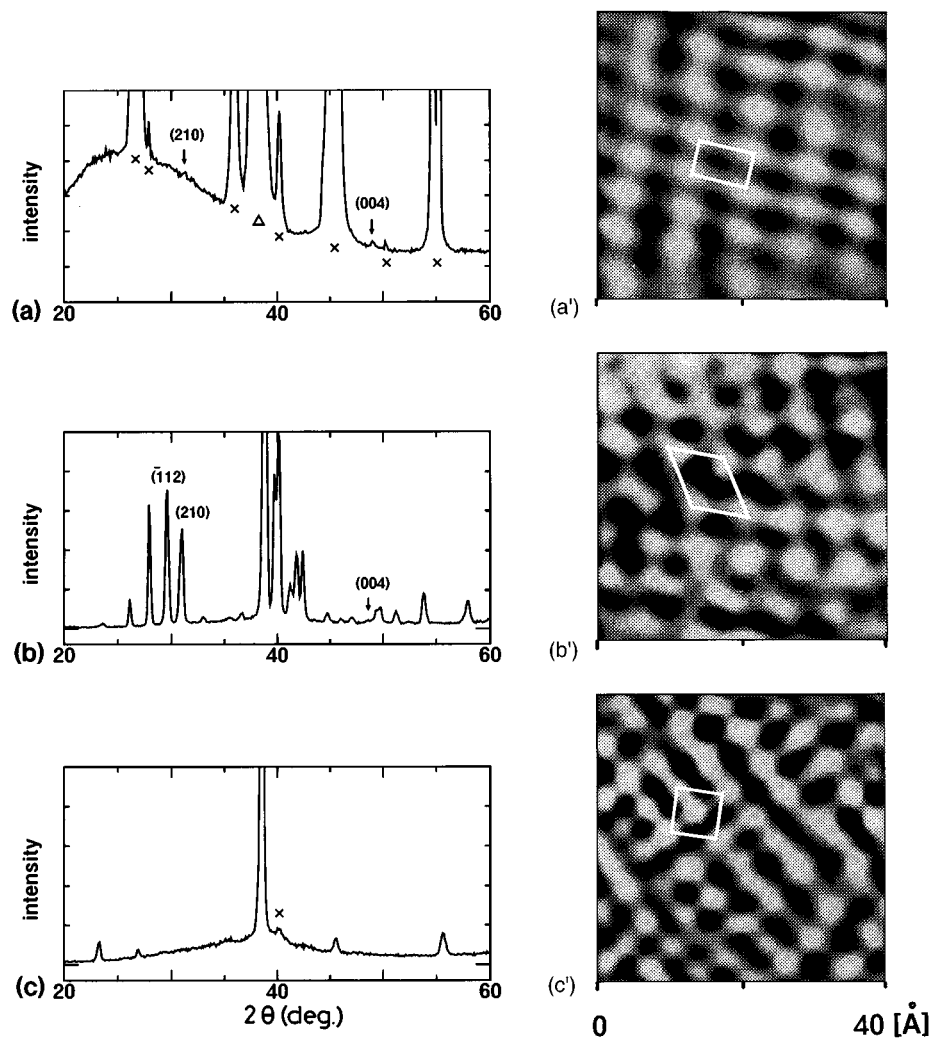


FIG. 1. X-ray diffraction patterns [(a), (b), (c)] and STM images [(a'), (b'), (c')] of  $\text{Ag}_2\text{Te}$  in a low-temperature phase film [(a), (a')], in low-temperature phase bulk [(b), (b')], and in high-temperature phase bulk [(c), (c')]. The STM images are  $40 \text{ \AA} \times 40 \text{ \AA}$  in size. (a), (a') are taken for a film at  $20 \text{ }^\circ\text{C}$ . In (a), peaks pointed out by the arrows are diffracted from  $\text{Ag}_2\text{Te}$ , the crosses from mica substrate, and the triangle from Ag metal. A broad halo peak at  $2\theta \approx 25^\circ$  is due to slide glass which holds the sample. In (a'), the solid line indicates a (001) monoclinic unit cell. (b), (b') are taken for bulk at room temperature. In (b), all the peaks can be indexed due to monoclinic  $\text{Ag}_2\text{Te}$ , while only three peaks are denoted. In (b'), the solid line indicates a (010) monoclinic unit cell. (c), (c') are taken for bulk at  $170 \text{ }^\circ\text{C}$ . In (c), the cross indicates the Al(111) peaks originating from the sample holder. In (c'), the solid line indicates a (100) cubic unit cell.

Here, we want to point out the high peak intensity arising from (004) surfaces in  $\text{Ag}_2\text{Te}$ . That is, the (004) peak in the figure is about ten times stronger than that expected for powder sample in which the intensity ratio between (004) and (210) is 6:100 [see Fig. 1(b)].<sup>13</sup> This strong (004) intensity suggests the (001) orientation of  $\text{Ag}_2\text{Te}$  crystallites in the film. Note that (001) and (002) peaks cannot appear because these are much weaker.<sup>4,13</sup>

Figure 1(a') shows a surface atomic structure of a film sample probed at  $20 \text{ }^\circ\text{C}$ . This image is taken using the constant current mode ( $V_s = -0.1 \text{ mV}$  and  $I_t = 2 \text{ nA}$ , where  $V_s$  is the sample voltage and  $I_t$  is the tunneling current); the time needed for scanning a frame is approximately 2 s. While the image is bandpass filtered in the Fourier spectrum, similar images can be obtained using only low-pass filters, confirming that the image is not artificial (this applies to other STM

images shown in the figure). Atomic features are clearly visible at bright spots in the gray scale. The averaged surface corrugation over some cross sections is  $\sim 0.7 \text{ \AA}$  in amplitude. A rectangular lattice ( $8.1 \text{ \AA} \times 4.5 \text{ \AA}$  in size), outlined in this figure is comparable to the (001) unit cell of the low-temperature phase  $\text{Ag}_2\text{Te}$ .<sup>4</sup> Note that this indexing is consistent with the film orientation inferred from the x-ray measurements. It is also noted that, in the film samples, only the patterns similar to Fig. 1(a') have been seen under many inspections, also consistent with the film orientation.

It is not known whether the bright spots observed are due to Ag or Te atoms. In compound semiconductors such as GaAs, atomic species are distinguishable by collecting the images at different polarity of tunneling bias voltages.<sup>14</sup> However, no clear voltage dependence has been seen in the present observations; similar images to that shown in Fig.

1(a') have been obtained at bias voltages of  $|V_s| \leq 10$  mV. It is known that Ag<sub>2</sub>Te is a degenerated semiconductor,<sup>6</sup> and accordingly the absence of the polarity dependence is understandable; that is, the electron tunneling can occur between extended electronic states in the tip and the conduction band in Ag<sub>2</sub>Te. Therefore, we cannot identify the origin of the bright spots. This argument also applies to the low-temperature phase in bulk samples shown in Fig. 1(b').

At bias voltages greater than  $\pm 0.2$  V no clear atomic structure is visible. The reason is speculative at present. The observations may imply deformable surface structures of superionic materials, possibly due to mobile Ag ions. In fact, holes and/or hillocks of a typical dimension of 50 nm have been observed reproducibly after application of voltages greater than  $\pm 1$  V. The details are under study.

At high temperatures, clear atomic images were not obtained in the film samples. Only atomic rows having a distance of  $\sim 5$  Å were detected at 162 °C. The results might be due to thermal drift.

Figures 1(b) and 1(c) show x-ray diffraction patterns of bulk Ag<sub>2</sub>Te powders in the low- and high-temperature phases. The measurements were performed at 20 °C (b) and 170 °C (c). The dramatic structural change seen is identified as the transition from the monoclinic lattice in the low-temperature phase to the cubic lattice in the high-temperature phase.<sup>4</sup> The phase-transition temperature of the bulk sample was found to be  $147 \pm 6$  °C by monitoring the intensity change of the  $(\bar{1}12)$  peak located at  $2\theta = 29.6^\circ$  [see Fig. 1(b)]. We also see in Fig. 1(c) a diffuse scattering peak centered at  $2\theta = 38^\circ$ , which has been interpreted as a signature of the disordered Ag lattice.<sup>4</sup>

An atomic structure of a cleaved surface of a bulk sample in the low-temperature phase is shown in Fig. 1(b'). This image was also taken under the constant current mode ( $V_s = -10$  mV and  $I_t = 1$  nA) at 20 °C and a frame-scan time of 2 s. The parallelogram lattice ( $9.0 \text{ Å} \times 8.1 \text{ Å}$ ) shown in the figure coincides with the unit cell of  $(0\bar{1}0)$  planes in the monoclinic Ag<sub>2</sub>Te. An averaged amplitude of the corrugation has been measured at  $\sim 0.7$  Å. In the case of the bulk sample, (001) atomic images, similar to Fig. 1(a'), have also been obtained for other cleaved surfaces.

Figure 1(c') shows an atomic image of the high-temperature phase Ag<sub>2</sub>Te at 170 °C. This image is taken using the constant height mode ( $V_s = +5$  mV and set-point of  $I_t = 1$  nA) and a frame-scan time of 1 s to minimize thermal drift. However, the measurement was still affected by thermal drift, and accordingly the image has been filtered.

To confirm the reliability of the image obtained at high temperatures, some additional investigations have been done. First, graphite surfaces were inspected under the same conditions; although somewhat noisy, they gave images with no appreciable distortion. Second, in order to confirm that the bias voltage acts just as a probe, a wider sample area was inspected after imaging a restricted region. No traces of the

previous monitoring have been found at  $|V_s| \leq 10$  mV. Third, the bias-voltage dependence was investigated. Images similar to that shown in Fig. 1(c') have been obtained at  $|V_s| \leq 10$  mV, while imaging has been impossible under higher bias voltages. The result implies deformable surface atoms of the superionic crystal.

We see in Fig. 1(c') a cubic lattice. It roughly coincides with a unit cell of the (100) surface of the high-temperature phase Ag<sub>2</sub>Te ( $6.6 \text{ Å} \times 6.6 \text{ Å}$ ) drawn in the figure. Since the lattice has a fcc structure, we can conclude that the bright spots are Te atoms. No traces of Ag atoms, which must be positioned randomly, have been obtained.

It is noted that in both the low- and high-temperature phases we cannot find any signatures of surface atomic reconstructions. Only the unit-cell structures of the bulk crystals have been obtained. It is known that the surface reconstruction is influenced by the ionicity of the chemical bonds in the material of interest.<sup>15</sup> In this context, Ag-Te bonds are highly ionic, and, thus the surface reconstruction is unlikely to take place.

#### IV. SUMMARY

Atomically resolved images of Ag<sub>2</sub>Te in the low- and high-temperature phases were obtained for the first time using film and bulk samples. In the low-temperature phase, (001) and  $(0\bar{1}0)$  surfaces of the monoclinic lattice were observed, and in the superionic high-temperature phase, (100) Te sublattices were imaged. Surface structural reconstruction was not observed in all the planes.

#### ACKNOWLEDGMENT

The authors thank T. Ishibashi for his technical support in x-ray diffraction measurements.

<sup>1</sup>Yu. Ya. Gurevich and A. K. Ivanov-Shits, in *Semiconductors and Semimetals*, edited by R. K. Willard and A. C. Beer (Academic, Boston, 1988), Vol. 26, pp. 338 and 342.

<sup>2</sup>S. Miyatani, *J. Phys. Soc. Jpn.* **14**, 996 (1959).

<sup>3</sup>M. Hansen, *Constitution of Binary Alloys* (McGraw-Hill, New York, 1958), pp. 55 and 57.

<sup>4</sup>J. Schneider and H. Schulz, *Z. Kristallogr.* **203**, 1 (1993).

<sup>5</sup>M. Kobayashi, K. Ishikawa, F. Tachibana, and H. Okazaki, *Phys. Rev. B* **38**, 3050 (1988).

<sup>6</sup>S. Miyatani, *J. Phys. Soc. Jpn.* **13**, 341 (1958).

<sup>7</sup>Y. Utsugi, *Nature* **347**, 747 (1990).

<sup>8</sup>Y. Utsugi, *Jpn. J. Appl. Phys.* **32**, 2969 (1993).

<sup>9</sup>E. Meyer and H. Heinzelmann, in *Scanning Tunneling Microscopy II*, edited by R. Wiesendanger and H.-J. Güntherodt (Springer, Berlin, 1992), pp. 133 and 139.

<sup>10</sup>H. Nozoye and H. Takada, *Jpn. J. Appl. Phys.* **33**, 3764 (1994).

<sup>11</sup>O. Rüdiger, *Ann. Phys.* **30**, 505 (1937).

<sup>12</sup>J. Schneir and P. K. Hansma, *Langmuir* **3**, 1025 (1987).

<sup>13</sup>*Powder Diffraction File (ASTM Card)*, edited by L. G. Berry (Joint Committee. Powder Diffraction Stand., Philadelphia, 1974).

<sup>14</sup>R. M. Feenstra, J. A. Stroscio, J. Tersoff, and A. P. Fein, *Phys. Rev. Lett.* **58**, 1192 (1987).

<sup>15</sup>M. Lannoo and P. Friedel, *Atomic and Electronic Structure of Surfaces* (Springer, Berlin, 1991), Chap. 5.